Estimation of Cone Index from Water Content and Soil Types Obtained from Hyperspectral Images

Norihiro Yamauchi[1], Shota Chikushi[1], Yusuke Tamura[1], Hiroshi Yamakawa[1]
Keiji Nagatani[1], Hiromitsu Fujii[2], Yuya Sakai[3], Takumi Chiba[3]
Shingo Yamamoto[3], Kazuhiro Chayama[3], Atsushi Yamashita[1], Hajime Asama[1]

Dept. of Precision Engineering[1]
The University of Tokyo
Tokyo, Japan

Dept. of Advanced Robotics[2]
Chiba Institute of Technology
Chiba, Japan

Fujita Corporation[3]
Tokyo, Japan

yamauchi@robot.t.u-tokyo.ac.jp

***Abstract*—In this study, it is aimed at non-contact judgment of traversability for construction machinery on weak ground. A new method for estimating cone index, one of the indicators of traversability, from discriminated soil types and estimated water content by hyperspectral cameras is proposed. Based on the initial experiments, there is a possibility to estimate cone index from hyperspectral images.**

***Index Terms*—traversability, cone index, hyperspectral image**

I. Introduction

Recently, landslide disasters occur frequently. After such disasters, prompt restoration work is necessary, and construction machinery is typically used for the work. Before introducing construction machinery in such environments, it is necessary to investigate traversability for the machinery, not to get stuck in weak ground. When the soil is too weak to support construction machinery, it may fall over and break down. Therefore, the restoration work may fail without traversability investigation. Generally, traversability is judged by workers on site. However, due to the risk of secondary disasters, workers had better not to enter landslide disaster sites. Therefore, unmanned traversability investigation is necessary. Teleoperated robots were used for unmanned traversability investigations [1] [2]. These robots measured cone index, which is one of the indicators of traversability of construction machinery. However, the above methods took very long time to measure cone index. Because these methods were contact type investigation method and required to make a measuring device contact soil at every measuring point. To reduce the time for the investigation, a non-contact type traversability investigation method is desired. Infrared images were used for non-contact cone index estimation methods [3] [4]. In these methods, water content was estimated from infrared wavelength to estimate cone index. These methods reduced the investigation time, because the investigation required only image shooting at the site. However, these methods only estimated water content and did not discriminate soil types that also affect cone index. It is known that cone index depends not only on water content, but also on soil types. Therefore, in this study, a new method to estimate cone index from water content for each soil type is proposed. The new method uses hyperspectral images in order to estimate not only water content, but also soil types. The hyperspectral images obtain spectral reflectance, which varies with soil types and water content.

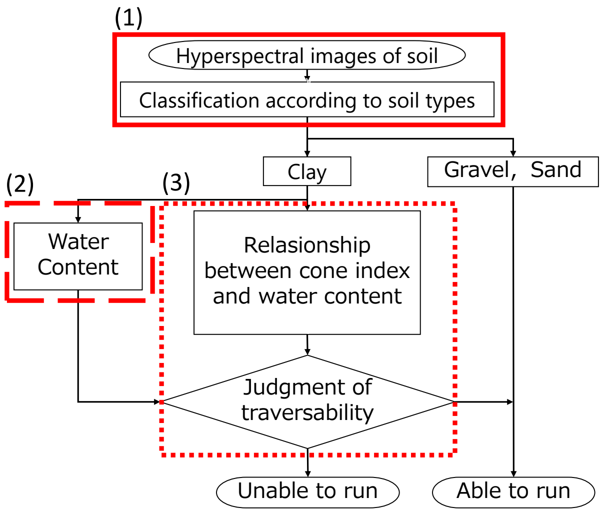

Fig. 1. Flowchart of traversability investigation

II. Methodology

The proposed traversability investigation method consists of three steps: step (1), step (2), and step (3). Figure 1 shows each step and the overview of the traversability investigation. In the step (1), soil types are discriminated from hyperspectral images. In the step (2), water content of clay is estimated from the hyperspectral images. In the step (3), cone index of clay is estimated from water content for each soil type.

In the step (1), to discriminate soil types from hyperspectral images, a neural network is used. Neural networks can automatically learn important features for the classification of hyperspectral images [5]. Therefore, in this step, soil types

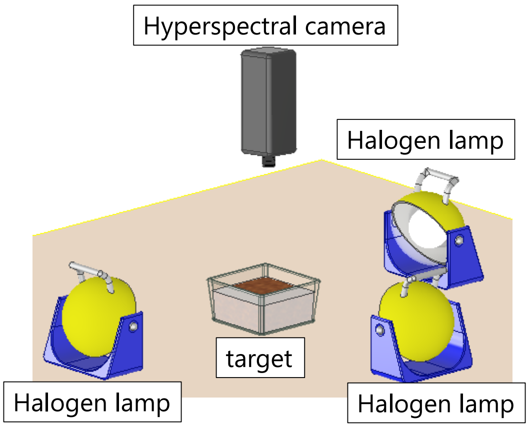

Fig. 2. Experiment overview

Fig. 3. An example of hyperspectral images

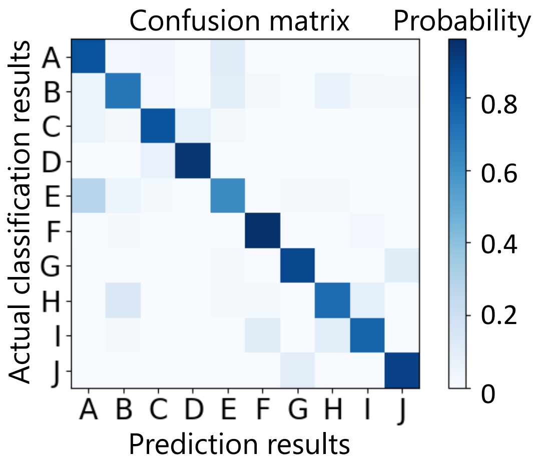

Fig. 4. Confusion matrix of hyperspectral images discrimination

are discriminated from hyperspectral images using the neural network with pre-learned images. As the result of this discrimination, hyperspectral images are classified into three soil groups: clay, sand, and gravel. It is known that the sand and the gravel can be traversed by construction machinery regardless of water content [6]. On the other hand, traversability of the clay is affected by water content. Therefore, water content is estimated when the soil type is classified into the clay.

In the step (2), water content is estimated from the gradient of the spectral reflectance spectrum which is obtained from hyperspectral images. Water absorbs light around 1450 nm. When the water content is 0, in wavelength from the visible to around 1450 nm, spectral reflectance increases as the wavelength increases. However, as the water content increases, spectral reflectance decreases. Therefore, as the water content increases, the gradient at 1450 nm decreases. In this study, water content is estimated by linear and exponential regressions from the gradient. The gradient of 1450 nm is obtained by calculating the first derivative of the spectral reflectance spectrum. The first derivative is calculated approximately from the difference between the spectral reflectance of 1440 nm and 1460 nm.

In the step (3), cone index of clay is estimated from water content for each soil type. Basically, cone index depends on soil types and water content. Therefore, if cone index for each water content and each soil type is known, the estimation of cone index is possible from soil types, water content, and the known cone index. When the soil type is discriminated in the step (1), the known cone index for each water content can be used. From the water contents recorded with the known corn index, two water contents immediately before and after the estimated one in the step (2) can be extracted. By dividing the two water contents internally with the estimated one, the internal ratio is calculated. Estimated cone index is the point which divides cone indexes corresponding to the extracted two water contents internally with the internal ratio calculated above.

III. Experiment

A. Experiment setup

Figure 2 shows an overview of the experiment. In this study, hyperspectral cameras, NH-7 and SIS-I manufactured by Eva Japan Co., Ltd., were used to take hyperspectral images. Figure 3 shows an example of the hyperspectral images used in this study. The images were taken indoors and we used halogen lamps as light sources. The reason for using them is to get all wavelengths of light acquired by the hyperspectral camera. 3 hyperspectral images were taken for each soil type. Among the 3 images, 2 images were used to learn the neural network to discriminate soil types and to make estimation equations of water content, and the remaining 1 image was used as test data for the discrimination of soil types and the estimation of water content. Hyperspectral images of 10 soil types were used. They were collected at 10 different locations. Among these 10 soil types, soil A, soil B, soil D, soil F, and soil G were clay. The rest of the soil types were sand or the gravel.

B. Results

1) Discrimination of soil types: Figure 4 shows the confusion matrix of the hyperspectral image discrimination of

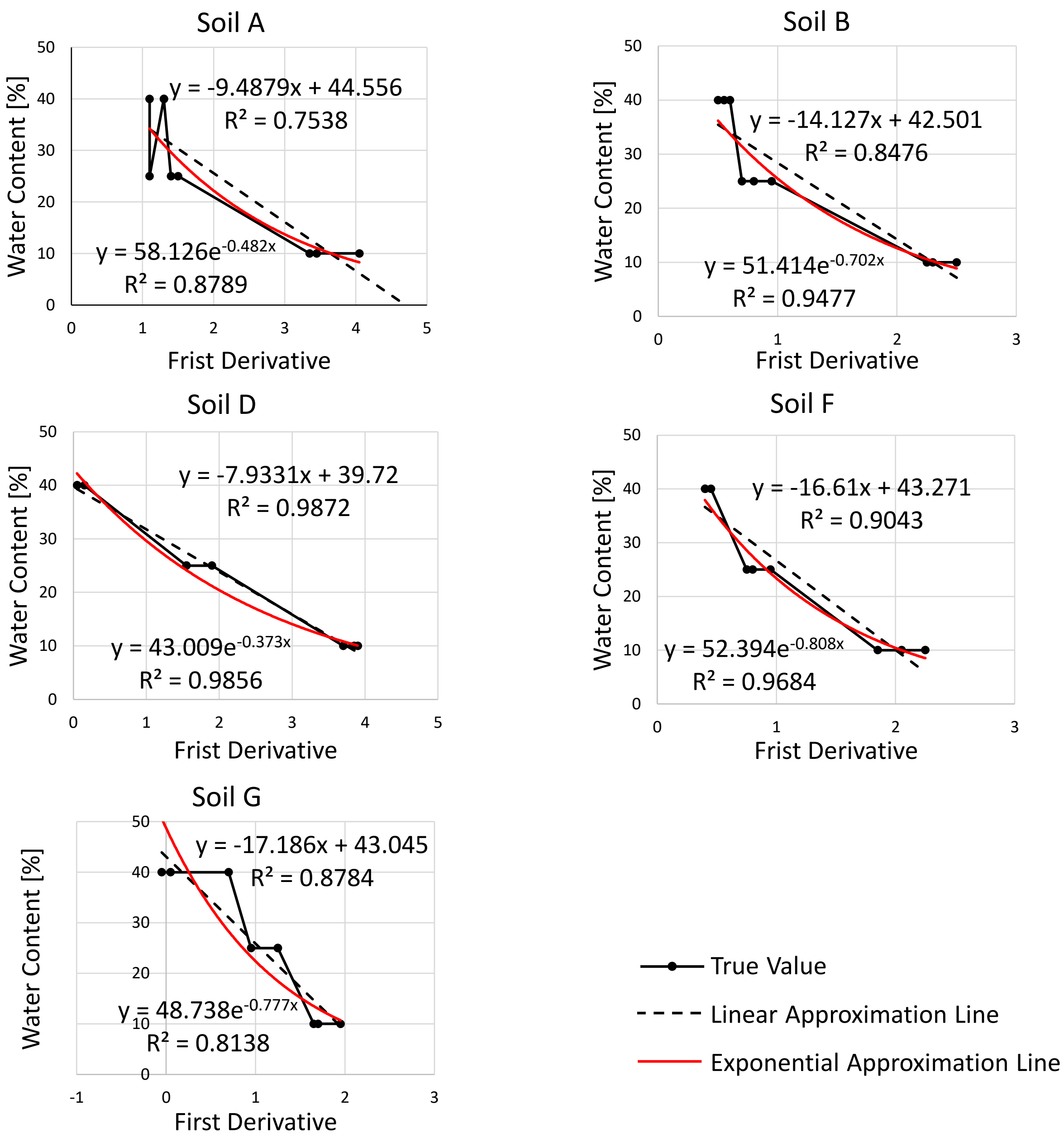

Fig. 5. Relationship between water content and the gradient of spectral reflectance around 1450nm.

the 10 soil types obtained in this experiment. The accuracy rate of the discrimination was 81.57 % for the test data. The discrimination of the 10 soil types from hyperspectral images was successful. From the result, it was found that the non-contact discrimination of soil types was possible by distinguishing the difference in the spectral reflectance spectrum depending on soil types.

2) Estimation of water content: Figure 5 shows the result of the water content estiamtion of clay: soil A, soil B, soil D, soil F, and soil G. In each graph, the horizontal axis shows the first derivative of the spectral reflectance spectrum. On the other hand, the vertical axis shows the water content. In the graphs, the black solid lines show the relationship between the measured water content and the spectral reflectance gradient, and black dotted lines and red solid lines are linear approximation lines and exponential approximation lines to the above-mentioned black solid lines respectively. In these graphs, the linear approximation lines and the exponential approximation lines were along the actually measured black solid lines. Using the approximation line equations, calculation

TABLE I
ESTIMATED CONE INDEX FROM ESTIMATED WATER CONTENT FOR EACH SOIL TYPE

soil group	soil type and water content	estimated soil type	estimated water content	calculated cone index
clay	Soil A 10 %	A	10.26 %	4333 kN/m^2
	Soil A 40 %	A	29.20 %	401 kN/m^2
	Soil B 10 %	B	9.51 %	12405 kN/m^2
	Soil B 40 %	B	27.88 %	6344 kN/m^2
	Soil D 10 %	D	6.97 %	1664 kN/m^2
	Soil D 40 %	D	37.98 %	237 kN/m^2
	Soil F 10 %	F	10.67 %	9298 kN/m^2
	Soil F 40 %	F	35.70 %	7570 kN/m^2
	Soil G 10 %	G	11.76 %	6460 kN/m^2
	Soil G 40 %	G	37.87 %	2 kN/m^2
gravel or sand	Soil C 10 %	C		
	Soil C 40 %	C		
	Soil E 10 %	E		
	Soil E 40 %	E		
	Soil H 10 %	H		
	Soil H 40 %	H		
	Soil I 10 %	I		
	Soil I 40 %	I		
	Soil J 10 %	J		
	Soil J 40 %	J		

of estimated water contents from the first derivatives of the spectral reflectance spectrum of 1450 nm was successful. From the result, it was found that estimation of water content was possible by the fact that the spectral reflectance at water absorption wavelength band decreases as the water content increases.

3) Calculation of cone index: Table I shows the result of the estimation of water content, estimation of soil types, and calculation of the estimated cone index. Water content and soil types were estimated for only clay: soil A, soil B, soil D, soil F, and soil G. The leftmost column shows the soil group and the second column from the left shows the true soil type and water content of each soil type. The remaining columns show the discriminated soil types, estimated water content, and estimated cone index, respectively. The columns of the discriminated soil types and estimated water content show the result of the step (1) and the step (2) respectively. From this table, it was found that the calculation of the estimated cone index of clay from hyperspectral images was possible. This estimation assumes that cone index depends on soil types and water content. In order to confirm whether the assumption can be used, it is necessary to compare the actual measured cone index and the estimated one by the proposed method.

IV. CONCLUSION

In this study, a new method to estimate cone index of clay from hyperspectral images for evaluation of traversability of construction machinery is proposed. According to the initial experiments, the soil types and water content were estimated from hyperspectral images, and estimation of cone index from hyperspectral images was possible. In the future, it will be required to compare an actually measured cone index with an estimated one by the proposed method in this study to validate the method.

ACKNOWLEDGMENT

This work was in part supported by JSPS KAKENHI Grant Number JP18K13810.

REFERENCES

[1] S. Chhaniyara, C. Brunskill, B. Yeomans, M. C. Matthews, C. Saaj, S. Ransom and L. Richter, “Terrain Trafficability Analysis and Soil Mechanical Property Identification for Planetary Rovers: A Survey”, *Journal of Terramechanics*, vol. 49, pp. 115–128, Feb. 2012.

[2] K. Zacny, J. Wilson, J. Craft, V. Asnani, H. Oravec, C. Creager, J. Johnson and T. Fong, “Robotic Lunar Geotechnical Tool”, *Proceeding of the 2010 ASCE Earth and Space, Honolulu, HI*, Mar. 2010.

[3] R. Fernández, H. Montes and C. Salinas, “VIS-NIR, SWIR and LWIR Imagery for Estimation of Ground Bearing Capacity”, *Sensors*, pp. 13994–14015, Jun. 2015.

[4] A. L. Rankin, and L. H. Matthies, “Passive Sensor Evaluation for Unmanned Ground Vehicle Mud Detection”, *Journal of Field Robotics*, vol. 27, no. 4, pp. 473–490, Mar. 2010.

[5] Wei Hu, Yangyu Huang, Li Wei, Fan Zhang and Hengchao Li, “Deep Convolutional Neural Networks for Hyperspectral Image Classification”, *Journal of Sensors*, vol. 2015, pp. 1–12, Jan. 2015.

[6] M. P. Meyer and S. J. Knight, “Trafficability of Soil Soils classification”, U.S. Army Engineer Waterways Experiment Station Corps of Engineers, Vicksburg, Mississippi, Technical Memorandum no. 3-240, sixteenth supplement. pp. 1–182, Aug. 1961.